0026-895X/11/7903-389–399$20.00
MOLECULAR PHARMACOLOGY
Vol. 79, No. 3
69120/3668122
Mol Pharmacol 79:389–399, 2011
Printed in U.S.A.

THRX-198321 Is a Bifunctional Muscarinic Receptor Antagonist and β_2-Adrenoceptor Agonist (MABA) That Binds in a Bimodal and Multivalent Manner

Tod Steinfeld, Adam D. Hughes, Uwe Klein, Jacqueline A. M. Smith, and Mathai Mammen

Theravance, Inc., South San Francisco, California

Received September 29, 2010; accepted December 7, 2010

ABSTRACT

Biphenyl-2-yl-carbamic acid 1-{9-[(*R*)-2-hydroxy-2-(8-hydroxy-2-oxo-1,2-dihydro-quinolin-5-yl)-ethylamino]-nonyl}-piperidin-4-yl ester (THRX-198321) is a single molecule composed of a muscarinic acetylcholine receptor (mAChR) antagonist moiety, represented by the fragment MA, linked by a C9 polymethylene chain to a β_2-adrenoceptor (β_2AR) agonist moiety, represented by the fragment 8-hydroxy-5-((*R*)-1-hydroxy-2-methylamino-ethyl)-1*H*-quinolin-2-one (BA). THRX-198321 exhibited high affinity for mAChR (M_2 $pK_{I,App}$ = 10.57 ± 0.09; M_3 $pK_{I,App}$ = 10.07 ± 0.11) and β_2AR ($pK_{I,App}$ = 9.54 ± 0.15), with potent mAChR antagonist (M_2 $pK_{I,Fn}$ = 9.69 ± 0.23; M_3 $pK_{I,Fn}$ = 10.05 ± 0.17) and β_2AR agonist (pEC_{50} = 9.25 ± 0.02) activities. Consistent with multivalent interactions, THRX-198321 binding affinity was >300-fold higher at mAChR and 29-fold higher at β_2AR relative to its monovalent fragments biphenyl carbamic acid piperidinyl ester (MA) and BA, respectively. THRX-198321 was a competitive antagonist at mAChR (M_2 pK_B = 9.98 ± 0.13; M_3 pK_B = 10.31 ± 0.89), whereas THRX-198321 agonist activity at β_2AR was competitively inhibited by propranolol. Interactions of THRX-198321 with an allosteric site on mAChR and a novel extracellular allosteric site on β_2AR, respectively, were detected by measuring THRX-198321-evoked changes in the dissociation rates for the orthosteric radioligands, [*N*-methyl-^{3}H]scopolamine methyl chloride (M_2 $pEC_{50,diss}$ = 6.73 ± 0.10; M_3 $pEC_{50,diss}$ = 5.02 ± 0.14) and [4,6-propyl-^{3}H]dihydroalprenolol (β_2AR $pEC_{50,diss}$ = 3.82 ± 0.25). The carbostyril-linker fragment (BA-L) binds to the allosteric site of mAChR (M_2 $pEC_{50,diss}$ = 5.06 ± 0.03; M_3 $pEC_{50,diss}$ = 4.15 ± 0.25), whereas the MA fragment binds to the allosteric site of β_2AR ($pEC_{50,diss}$ = 3.60 ± 0.18). Collectively, these observations suggest that THRX-198321 exhibits a multivalent bimodal orientation in the orthosteric and allosteric binding pockets of mAChR and β_2AR, a phenomenon that may be unique to this class of molecule.

Introduction

Chronic obstructive pulmonary disease (COPD) is a leading cause of morbidity and mortality throughout the world and is predicted to become the fourth leading cause of death by 2030 and the third leading cause of chronic disability by 2020 (Mathers and Loncar, 2006). Bronchodilators, such as mAChR antagonists and β_2AR agonists, are important treatment options given their ability to improve airflow and reduce the number of exacerbations (Calverley, 2004; Baker et al., 2009). Several studies have shown that drugs from these classes are effective alone but achieve greater efficacy when administered in combination (Cazzola et al., 2004; Baloira Villar and Vilariño Pombo, 2005; van Noord et al., 2005, 2006; Aaron et al., 2007; Tashkin et al., 2008). A single molecule that exhibits both mAChR antagonist and β_2AR agonist (MABA) activity may offer several advantages over combination therapy of two drug entities. These include a single pharmacokinetic profile, a uniform ratio of activities at the cellular level, and a simplified clinical development program. In addition, the potential exists for combination with an inhaled corticosteroid to offer "triple" therapy in a single inhalation delivery device.

Article, publication date, and citation information can be found at http://molpharm.aspetjournals.org.
doi:10.1124/mol.110.069120.

ABBREVIATIONS: β_2AR, β2-adrenoceptor; mAChR, muscarinic acetylcholine receptor; MABA, mAChR antagonist and β_2AR agonist; THRX-160209, 4-{*N*-[7-(3-(*S*)-(1-carbamoyl-1,1-diphenylmethyl)pyrrolidin-1-yl)hept-1-yl]-*N*-(*n*-propyl)amino}-1-(2,6-dimethoxybenzyl)piperidine; THRX-198321, biphenyl-2-yl-carbamic acid 1-{9-[(*R*)-2-hydroxy-2-(8-hydroxy-2-oxo-1,2-dihydro-quinolin-5-yl)-ethylamino]-nonyl}-piperidin-4-yl ester; NMS, *N*-methyl-scopolamine methyl chloride; DHA, 4,6-propyl-dihydroalprenolol; W84, 3-Methyl-5-[7-[4-[(4*S*)-4-methyl-1,3-oxazolidin-2-yl]phenoxy]heptyl]-1,2-oxazole; MA, biphenyl carbamic acid piperidinyl ester; MA-L, biphenyl-2-yl-carbamic acid 1-nonyl-piperidin-4-yl ester; BA, 8-hydroxy-5-((*R*)-1-hydroxy-2-methylamino-ethyl)-1*H*-quinolin-2-one; BA-L, 8-hydroxy-5-((*R*)-1-hydroxy-2-nonylamino-ethyl)-1*H*-quinolin-2-one; HTRF, homogeneous time-resolved fluorescence; CHO, Chinese hamster ovary; HEK, Human embryonic kidney; PBS, phosphate-buffered saline; IP_1, myoinositol-1-phosphate; GTPγS, guanosine 5′-*O*-(3-thio)triphosphate; BSA, bovine serum albumin.

We hypothesized that it was possible to discover a molecule exhibiting dual mAChR and β_2AR pharmacology using a multivalent design strategy (Griffin et al., 2003; Smith et al., 2006; Steinfeld et al., 2007; Long et al., 2008; McKinnell et al., 2009). In addition to dual pharmacology, a multivalent ligand is predicted to offer enhanced binding affinity and target specificity relative to its monovalent equivalents (Mammen et al., 1998a,b). Multivalent binding refers to the interaction of multiple binding motifs on a ligand with adjacent concavities on a single target receptor (intramolecular binding) or on adjacent target receptors (intermolecular binding). Two such adjacent binding pockets on a single target may be an orthosteric binding site and a nearby secondary, or allosteric modulator, site. Allosteric modulators are ligands that bind to sites that are topographically distinct from the primary ligand, or orthosteric, site and may change the conformation of the receptor such that orthosteric ligand affinity and/or efficacy is altered (May et al., 2007). A novel concept for ligand binding to GPCRs is that of bimodal multivalent binding. Bimodal binding describes the reciprocal modes of binding at two different types of receptor. Thus, for a multivalent ligand composed of structural moieties A and B, at one receptor, A and B bind to orthosteric and allosteric sites, respectively, whereas at the second receptor, A and B bind to allosteric and orthosteric sites, respectively.

For a multivalent ligand to bind in a bimodal manner at two distinct receptors, the respective receptors should, ideally, each contain at least two binding pockets that are similar enough to accommodate the same ligand binding motifs and have a similar spatial relationship on each receptor. In addition to the ACh orthosteric binding site, mAChRs exhibit at least one nearby, yet topographically distinct, well characterized allosteric modulator site that binds mAChR allosteric ligands, such as gallamine, W84, and obidoxime (Tränkle and Mohr, 1997). We have demonstrated previously that 4-{*N*-[7-(3-(*S*)-(1-carbamoyl-1,1-diphenylmethyl)pyrrolidin-1-yl)hept-1-yl]-*N*-(*n*-propyl)amino}-1-(2,6-dimethoxybenzyl)piperidine (THRX-160209), a compound that exhibits simultaneous binding interactions at the orthosteric and "gallamine" allosteric sites of M_2 mAChR, is a high-affinity multivalent ligand with selectivity over all other mAChRs (Steinfeld et al., 2007).

Although norepinephrine may occupy a comparable orthosteric site on β_2AR, no known extracellular allosteric modulators sites have been described, to the best of our knowledge. A salmeterol "exosite" has been described and located on β_2AR; however, the interaction between the salmeterol aromatic ring and this site enhances receptor residency time and not affinity or potency (Green et al., 1996). Furthermore, no allosteric modulatory effects have been reported for this site. An intracellular Zn^{2+} binding site has been described for β_2AR (Swaminath et al., 2002, 2003), but this site is inaccessible to large, cell-impermeant ligands. Extracellular secondary sites or allosteric binding pockets may exist on β_2AR but these may have avoided detection because of tolerance of binding (i.e., allosteric ligand binding failing to modulate orthosteric ligand binding) or because modulatory effects are too modest to measure.

In the present study, we describe the pharmacological profile of a novel multivalent ligand that exhibits dual mAChR antagonist and β_2AR agonist pharmacologies (MABA). Biphenyl-2-yl-carbamic acid 1-{9-[(*R*)-2-hydroxy-2-(8-hydroxy-2-oxo-1,2-dihydro-quinolin-5-yl)-ethylamino]-nonyl}-piperidin-4-yl ester (THRX-198321) (Fig. 1) is a representative MABA that was the product of a multivalent design strategy targeting the orthosteric and allosteric sites on mAChR, the orthosteric site on β_2AR and a novel allosteric site on β_2AR, and was chosen as a tool for the present study. We provide evidence to suggest that the binding orientations for THRX-198321 at mAChR and β_2AR are bimodal.

Materials and Methods

Materials. [^{3}H]NMS (specific activity, 82 Ci/mmol) and [^{3}H]DHA (specific activity, 89 Ci/mmol) were obtained from GE Healthcare (Chalfont St. Giles, Buckinghamshire, UK). Atropine, oxotremorine, and isoproterenol were purchased from Sigma Chemical Co. (St. Louis, MO). 3-Methyl-5-[7-[4-[(4*S*)-4-methyl-1,3-oxazolidin-2-yl]phenoxy]heptyl]-1,2-oxazole (W84) and propranolol were purchased from Tocris Cookson, Inc. (Ellisville, MO). Obidoxime chloride was purchased from Toronto Research Chemicals (Toronto, ON, Canada). THRX-198321, biphenyl carbamic acid piperidinyl ester (MA), biphenyl-2-yl-carbamic acid 1-nonyl-piperidin-4-yl ester (MA-L), 8-hydroxy-5-((*R*)-1-hydroxy-2-methylamino-ethyl)-1*H*-quinolin-2-one (BA), and 8-hydroxy-5-((*R*)-1-hydroxy-2-nonylamino-ethyl)-1*H*-quinolin-2-one (BA-L), and various linker analogs of THRX-198321 (C7-C12) were prepared at Theravance. HTRF cAMP and IP-One assay kits were purchased from CisBio International (Bagnols sur Cèze, France).

Cell Culture and Membrane Preparation. Cells were grown under 5% CO_2 at 37°C. Chinese hamster ovary (CHO)-K1 cells stably

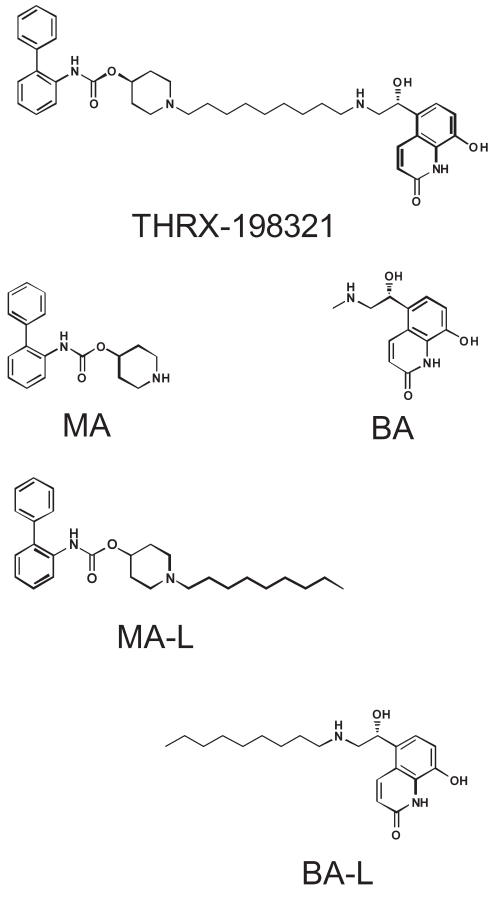

Fig. 1. Chemical structures of THRX-198321; monovalent fragments of THRX-198321, MA, and BA; and linker conjugated fragments MA-L and BA-L.

transfected with the human recombinant M_2 or M_3 mAChR were grown in Ham's F12 medium containing 10% fetal bovine serum and 250 μg/ml G-418 (Geneticin). Human embryonic kidney (HEK)-293 cells transfected with human recombinant β_2AR were grown in Dulbecco's modified Eagle's medium containing 10% fetal bovine serum and 250 μg/ml G-418. Cells were grown to confluence and harvested with phosphate-buffered saline (PBS) containing 5 mM EDTA. For intact cell assays, lifted cells were washed with PBS and used immediately. For membrane preparations, cells were suspended in ice-cold 10 mM HEPES with 10 mM EDTA, pH 7.4 (mAChR CHO-K1 cells) or ice-cold 75 mM Tris with 10 mM EDTA, pH 7.4 (β_2AR HEK-293 cells) and homogenized using a cell disrupter. The homogenate was sedimented by centrifugation (500*g*, 10 min). The supernatant was then centrifuged again (40,000*g*, 20 min), and the pellets were suspended in 10 mM HEPES buffer with 20 mM NaCl, pH 7.4 (mAChR CHO-K1 cell membranes) or 75 mM Tris buffer, pH 7.4 (β_2AR HEK-293 cell membranes) and stored at −80°C. These preparations typically yielded 2.4, 2.7, or 2.5 pmol/mg protein of β_2AR, M_2, or M_3 receptors, respectively, as determined using [^{3}H]DHA (for B2AR) or [^{3}H]NMS (for M2 or M3 mAChR) radioligand binding assays.

cAMP Accumulation Assay. To determine β_2AR agonist potencies, cAMP accumulation in HEK-293 cells expressing β_2AR was measured in white half-area 96-well microplates using the HTRF cAMP Dynamic kit (CisBio International). In brief, cells were stimulated for 15 min at 37°C with test compounds in PBS with the phosphodiesterase inhibitor 3-isobutyl-1-methylxanthine. Inhibition of the agonist response was measured in the presence of the β_2AR antagonist propranolol. The reaction was stopped with the addition of vendor-supplied lysis/conjugation buffer containing HTRF assay reagents: the d2-labeled cAMP, followed by the europium cryptate-labeled anti-cAMP antibody. The assay was incubated overnight at 20°C, and time-resolved fluorescence resonance energy transfer signals were measured 60 μs after excitation at 317 nm and emission at 585 and 665 nm using a Safire^2 instrument (Tecan Group Ltd, Männedorf, Switzerland). Ratios of relative fluorescence units (RFU) measured at each wavelength ($10^4 \times RFU_{665\ nm}/RFU_{585\ nm}$) were plotted against concentration of test compound and analyzed by nonlinear regression using a four-parameter logistic function in Prism 5.0 (GraphPad Software, San Diego, CA) to determine agonist EC_{50} values.

Myoinositol-1-Phosphate Accumulation Assay. To determine M_3 receptor antagonist potencies, myoinositol-1-phosphate (IP_1) accumulation in CHO-K1 cells expressing M_3 mAChR was measured in 96-well microplates using the HTRF IP-One terbium assay kit (CisBio International). In brief, cells were stimulated for 2 h at 37°C with the mAChR agonist oxotremorine in the presence or absence of test ligands by using the vendor-supplied stimulation buffer. The reaction was stopped by the addition of vendor-supplied lysis/conjugation buffer containing HTRF assay reagents: the d2-labeled IP_1, followed by the terbium cryptate-labeled anti-IP_1 antibody. The assay was incubated overnight at 20°C, and time-resolved fluorescence resonance energy transfer signals were measured as described above. Data were analyzed by nonlinear regression using a four-parameter logistic function in Prism 5.0 to determine antagonist IC_{50} values. Slope factors were not different from unity, and therefore, antagonist $pK_{I,Fn}$ values were calculated from IC_{50} values, (Cheng and Prusoff, 1973) using the oxotremorine EC_{50} and concentration.

[^{35}S]GTPγS Binding Assay. To determine M_2 antagonist potencies, inhibition of oxotremorine-stimulated [^{35}S]GTPγS binding to CHO-K1 cell membrane fractions expressing M_2 mAChR was measured. Test compound and 0.5 μM oxotremorine were incubated together with membranes for 1 h in assay buffer consisting of 10 mM HEPES with 20 mM NaCl and 0.025% BSA, pH 7.4, at 20°C. A second 1-h incubation period followed the addition of 3 μM GDP and 0.4 nM [^{35}S]GTPγS. Membranes were then collected on 0.1% BSA pretreated GF/B filter plates (PerkinElmer Life and Analytical Sciences, Waltham, MA) via rapid filtration. Bound radioligand was measured by scintillation counting and cpm data were analyzed using a four-parameter logistic equation using Prism 5.0. The slopes of oxotremorine response curves were not equal to unity; therefore, antagonist inhibition constants ($K_{I,Fn}$) values were calculated from IC_{50} values using the equation

$$K_{I,Fn} = \frac{IC_{50}}{(2 + ([A]/EC_{50})^n)^{1/n} - 1}$$

where [A] is the oxotremorine concentration and n is the slope factor (Leff and Dougall, 1993).

Dissociation Kinetics Assays. mAChR ligand dissociation assays were performed as described previously (Steinfeld et al., 2007). Membrane fractions expressing mAChR or β_2AR were labeled with 0.5 nM [^{3}H]NMS or 0.5 nM [^{3}H]DHA, respectively, for 1 h at 20°C in 10 mM HEPES, 20 mM NaCl, or 75 mM Tris buffer. In addition, some studies were conducted using intact HEK-293 cells expressing β_2AR in an isotonic buffer consisting of 75 mM Tris and 3.5% D-mannitol supplemented with 1% BSA or 1 mM EDTA. In these studies, cell integrity was confirmed before and after each experiment by trypan blue staining. After equilibrium with the radioligand was established, 10 μM atropine (mAChR) or 10 μM propranolol (β_2AR) was added at various time points to prevent reassociation of the radioligand with the receptor. Additions were made in the presence or absence of test compound and, in the case of M_2 mAChR, with or without obidoxime. Membrane preparations or cells were collected onto 0.3% polyethylenimine-treated GF/B filter plates and radioactivity was measured by scintillation counting. Data (cpm) were normalized to percentage of total specific binding and analyzed using the monoexponential decay function in Prism 5.0 to derive the apparent dissociation rate constants in the presence of each concentration of allosteric modulator (k_{obs}). The apparent rate constant was then expressed as a percentage of the apparent rate constant for the radioligand determined in the absence of allosteric modulator (k_{off}). The data (k_{obs}/k_{off}, percentage) were then plotted versus ligand concentration and analyzed by nonlinear regression to calculate allosteric modulator $pEC_{50,diss}$ values or the negative log of the concentration required to retard the orthosteric radioligand dissociation rate by 50%.

Inhibition Radioligand Binding Assay. Inhibition radioligand binding assays were conducted with 0.5 nM [^{3}H]NMS in a 10 mM HEPES buffer containing 20 mM NaCl and 0.025% BSA, pH 7.4, at 20°C (mAChR) or with 0.5 nM [^{3}H]DHA in a 75 mM Tris buffer containing 0.025% BSA, pH 7.4, at 20°C (β_2AR). Nonspecific binding was defined in the presence of 10 μM atropine or 10 μM propranolol (mAChR or β_2AR, respectively). Membrane fractions were incubated with radioligand and unlabeled test compounds for 2 h at 20°C. After separation by vacuum filtration onto GF/B filter plates presoaked with polyethylenimine, the quantity of membrane-bound radioligand was measured by scintillation counting. Data (cpm) were normalized to percentage specific binding and analyzed using a four-parameter logistic equation in Prism 5.0. Hill coefficients did not differ significantly from unity; therefore, IC_{50} values were determined with slopes fixed to unity. Apparent K_I values ($K_{I,App}$) were calculated from the IC_{50} values (Cheng and Prusoff, 1973).

Competitive Interactions Analyses. Antagonist-induced rightward shifts of concentration-response curves were analyzed by nonlinear regression (Lew and Angus, 1995) to check for competitive interactions and calculate pK_B or pA_2 values for the antagonist. Data were also plotted according to the method of Arunlakshana and Schild (1959) for visualization.

Statistics. Data are presented as mean ± S.D., unless otherwise noted. For antagonist regression analyses, values are reported as pK_B or pA_2 ± S.D. When checking for a competitive interaction between agonist and antagonists, fits to the various nonlinear regression models were compared using an F test. The statistical

significance of differences between values was determined using a student's t test. Differences were considered to be statistically significant for $p < 0.05$.

Results

MABA Potencies and Orthosteric Site Interactions Measured by Functional In Vitro Assays. In HTRF inositol phosphate studies designed to measure functional antagonist activity in cells expressing M_3 mAChR, THRX-198321 inhibited oxotremorine-stimulated turnover of inositol phosphates in a concentration-dependent manner ($pK_{I,Fn} = 10.05 \pm 0.17$). Furthermore, increasing concentrations of THRX-198321 or the MA fragment shifted oxotremorine concentration-response curves to the right in a parallel fashion. Curve shifts were analyzed by nonlinear regression models (Lew and Angus, 1995) in which oxotremorine pEC_{50} values were plotted against the concentrations of the antagonist (Fig. 2, A and B). Data for THRX-198321, MA, and atropine were best fit to the model that is analogous to a linear Schild plot with a slope of unity. These data suggest a competitive interaction between oxotremorine and THRX-198321, MA and atropine. pK_B values of 10.31 ± 0.89, 7.05 ± 0.52, and 8.58 ± 0.26 were calculated for THRX-198321, MA, and atropine, respectively (Table 1). To more easily visualize the data, curves shifts are represented as Schild plots (Fig. 2, C and D).

THRX-198321, MA, and MA-L inhibited oxotremorine-stimulated [^{35}S]GTPγS binding via M_2 receptors in a concen-

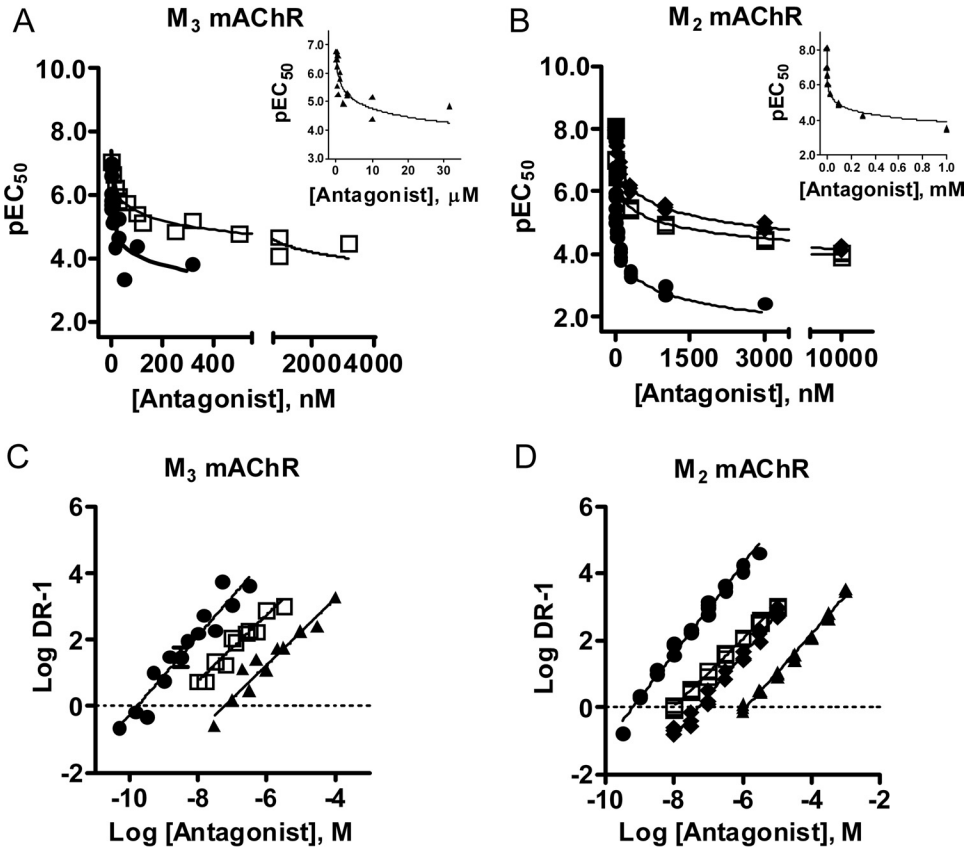

Fig. 2. Inhibition of agonist stimulated mAChR activity. Antagonist-induced rightward shifts of oxotremorine-stimulated inositol phosphate turnover (IP_1 accumulation) via M_3 mAChR expressed in CHO-K1 cells (A) or oxotremorine-stimulated [^{35}S]GTPγS binding via M_2 mAChR expressed in CHO-K1 cell membranes (B) were analyzed using nonlinear regression (Lew and Angus, 1995). For visualization, curve shifts were expressed as dose ratios (DR) in the form of a Schild plot (C, M_3 mAChR IP_1 accumulation; D, M_2 [^{35}S]GTPγS binding). A, inset, M_3 IP_1 accumulation for MA using a micromolar scale. B, inset, M_2 mAChR [^{35}S]GTPγS binding for MA using a millimolar scale. Data for mAChR antagonists THRX-198321 (●), MA (▲), MA-L (♦), or atropine (□) are from three separate experiments performed in duplicate.

TABLE 1

Functional inhibition constants ($pK_{I,Fn}$) and pA_2 values at M_2 and M_3 mAChR and β_2AR potencies (pEC_{50}) for THRX-198321 and THRX-198321 fragments

Antagonist and agonist potencies at CHO-K1 cell membranes expressing M_2 mAChR, CHO-K1 cells expressing M_3 mAChR, and HEK-293 cells expressing β_2AR were determined using conventional [^{35}S]GTPγS, HTRF IP-One terbium, or HTRF cAMP assays, respectively. Mean pK_I or pEC_{50} (± S.D.) values are from three separate experiments, each performed in duplicate. pK_B or pA_2 (± S.E.M.) values are derived from at least four separate experiments.

	M_2		M_3		β_2AR pEC_{50}	Propranolol β_2AR pK_B or pA_2
	$pK_{I,Fn}$	pK_B or pA_2	$pK_{I,Fn}$	pK_B or pA_2		
THRX-198321	9.69 ± 0.23	9.98 ± 0.13[a]	10.05 ± 0.17	10.31 ± 0.89[b]	9.25 ± 0.02	8.41 ± 0.11[b]
MA	7.62 ± 0.16	6.79 ± 0.07[a]	7.02 ± 0.15	7.05 ± 0.52[b]	<5	N.D.
MA-L	7.87 ± 0.24	7.95 ± 0.07[a]	7.76 ± 0.28	N.D.	<5	N.D.
BA	<5	N.D.	6.19 ± 0.25	N.D.	8.66 ± 0.12	8.63 ± 0.24[a]
BA-L	5.71 ± 0.21	N.D.	6.21 ± 0.25	N.D.	8.75 ± 0.31	N.D.
Atropine	8.83 ± 0.05	9.05 ± 0.04[b]	8.69 ± 0.21	8.58 ± 0.26[b]	N.D.	N.D.
Isoproterenol	N.D.	N.D.	N.D.	N.D.	9.22 ± 0.27	8.67 ± 0.27[a]

N.D., not determined.
[a] Slope factors were significantly different from unity and were a fitted parameter to calculate a pA_2 value using the Lew and Angus (1995) nonlinear regression model.
[b] Slope factors did not differ from unity and were fixed to 1 to calculate a pK_B value using the Lew and Angus (1995) nonlinear regression model.

tration-dependent manner. Slopes for oxotremorine concentration-response curves differed from unity (ranging from 0.62 to 0.84), and so $pK_{I,Fn}$ values were calculated from antagonist IC_{50} values using the Leff and Dougall (1993) correction. M_2 $pK_{I,Fn}$ values for THRX-198321, MA, and MA-L, were 9.69 ± 0.23, 7.62 ± 0.16, and 7.87 ± 0.24, respectively. Antagonists evoked a rightward, parallel shift of the oxotremorine concentration-response curves. However, a pK_B was calculated only for atropine (pK_B = 9.05 ± 0.04). Slope factors for THRX-198321, MA, and MA-L differed from unity, and pA_2 values calculated from nonlinear regression analyses were 9.98 ± 0.13 (slope = 1.30 ± 0.04), 6.79 ± 0.07 (slope = 1.30 ± 0.03), and 7.95 ± 0.07 (slope = 1.17 ± 0.02), respectively. The steep slope factors determined for THRX-198321, MA, and MA-L suggest there may be some degree of positive cooperativity between agonist and antagonist. Alternatively, the steep slopes may be due to nonequilibrium conditions or partial overlapping binding regions for these ligands. Overall, these data suggest a competitive interaction between oxotremorine and THRX-198321 at M_2 receptors via the MA binding moiety. In contrast, fragments containing the carbostyril moiety (BA and BA-L) were weak inhibitors of agonist-stimulated [^{35}S]GTPγS binding via M_2 receptors (BA M_2 $pK_{I,Fn} < 5$; BA-L M_2 $pK_{I,Fn}$ = 5.71 ± 0.21).

THRX-198321 increased cAMP accumulation in HEK-293 cells expressing β_2AR in a concentration-dependent manner (pEC_{50} = 9.25 ± 0.02). Likewise, we observed agonist activity for the THRX-198321 fragment, BA (pEC_{50} = 8.66 ± 0.12). THRX-198321 and BA evoked full agonist responses, with intrinsic activities of 0.93 ± 0.17 and 0.90 ± 0.20, respectively, relative to isoproterenol. The activities of both agonists were inhibited by the β_2AR antagonist, propranolol. Increasing concentrations of propranolol resulted in parallel rightward shifts of THRX-198321, BA, and isoproterenol concentration-response curves. Nonlinear regression analysis of the resulting curve shifts revealed that the data for THRX-198321 best fit to the model analogous to a linear Schild plot with a slope equal to unity (propranolol pK_B = 8.41 ± 0.11; Fig. 3). For BA and isoproterenol, the curve-shift data fit best the model analogous to a linear Schild plot with a slope not equal to unity (BA propranolol pA_2 = 8.63 ± 0.24, slope = 1.21 ± 0.08; isoproterenol propranolol pA_2 = 8.67 ± 0.27, slope = 1.21 ± 0.10). Propranolol antagonist potencies (pA_2 or pK_B) were similar for each agonist and were within the range of potencies and binding affinities (8.3–9.0) reported by other groups (Arch et al., 1984; Smith and Teitler, 1999). Overall, these data indicate that the antagonist propranolol competitively inhibited the agonists THRX-198321, BA, and isoproterenol. Furthermore, these data suggest that THRX-198321 binds to site on β_2AR coincident with isoproterenol and propranolol via the BA binding moiety.

Allosteric Interactions Measured by Orthosteric Radioligand Dissociation Assays. Kinetic assays using excess competing orthosteric ligand were employed to study potential interactions of THRX-198321, or fragments of THRX-198321, with secondary binding sites on M_2 and M_3 mAChR and β_2AR. Typically, ligands that bind to the well-defined mAChR allosteric sites retard the dissociation rate of orthosteric radioligands. In the absence of test drug, dissociation of [^{3}H]NMS at M_3 was monophasic with a half-life ($t_{1/2}$) of 22.7 ± 6.7 min and a dissociation rate constant (k_{off}) of 0.030 ± 0.011 min^{-1}. In the presence of 100 μM THRX-198321, the observed dissociation rate for [^{3}H]NMS was reduced significantly (~20-fold) to 0.0014 ± 0.0006 min^{-1} ($t_{1/2}$ = 550 ± 180 min). Furthermore, THRX-198321 produced a concentration-dependent retardation of [^{3}H]NMS dissociation from membrane fractions expressing human M_3 mAChR ($pEC_{50,diss}$ = 5.02 ± 0.14) in a manner similar to that observed with the well characterized mAChR allosteric ligand W84 ($pEC_{50,diss}$ = 5.20 ± 0.07; Table 2). Dissociation curves were monophasic in the pres-

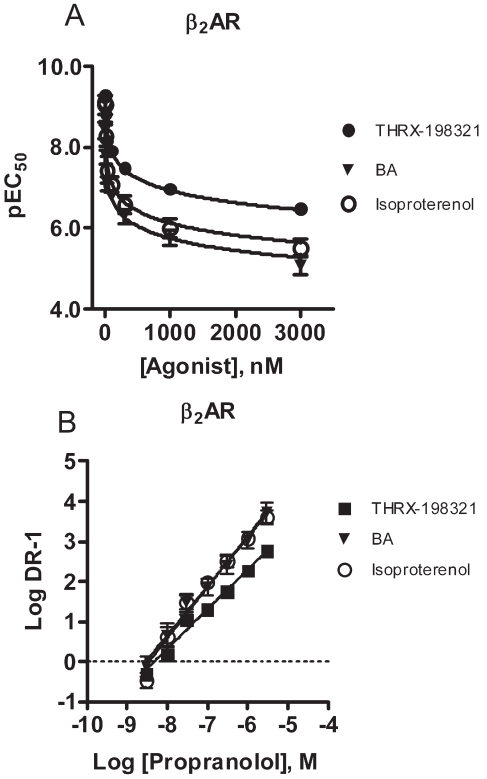

Fig. 3. Inhibition of agonist-stimulated β_2AR activity. A, agonist-stimulated cAMP accumulation in HEK-293 cells stably transfected with β_2AR was inhibited by propranolol. Propranolol-induced rightward shifts of agonist stimulated cAMP accumulation were analyzed using nonlinear regression (Lew and Angus, 1995). B, for visualization, curve shifts were expressed as dose ratios (DR) in the form of a Schild plot. β_2AR agonists THRX-198321 (●), BA (▼), or isoproterenol (○) were tested in three separate experiments performed in duplicate.

TABLE 2

Allosteric modulator potency ($pEC_{50,diss}$) values at M_2 and M_3 mAChR and β_2AR for THRX-198321 and THRX-198321 fragments

Data are expressed as $pEC_{50,diss}$ values (i.e. the negative log value of the concentration reducing radiolabeled orthosteric ligand dissociation rate by 50%). Retardation of [^{3}H]NMS dissociation rates at CHO-K1 cell membranes expressing M_2 mAChR or M_3 mAChR was measured following the addition of 10 μM atropine in the presence or absence of test compounds. Retardation of [^{3}H]DHA dissociation rates at HEK-293 cells expressing β_2AR was measured following the addition of 10 μM propranolol in the presence or absenc, of test compound. Data are mean values ± S.D. derived from four separate experiments.

	$pEC_{50,diss}$		
	M_2	M_3	β_2AR
THRX-198321	6.73 ± 0.10	5.02 ± 0.14	3.82 ± 0.25
MA	N.D.	N.D.	3.60 ± 0.18
BA	2.77 ± 0.08	2.73 ± 0.12	N.D.
BA-L	5.06 ± 0.03	4.15 ± 0.25	N.D.
W84	7.10 ± 0.09	5.20 ± 0.07	N.D.

N.D., not determined.

ence of all compounds studied (Fig. 4). These results are consistent with an allosteric interaction for THRX-198321 at M_3 mAChR.

The effects of THRX-198321 fragments on [^{3}H]NMS dissociation rates were also investigated. The fragment, BA, reduced the off-rate of [^{3}H]NMS from M_3 mAChR at concentrations higher than 100 μM. The M_3 receptor $pEC_{50,diss}$ for this fragment was determined to be 2.73 ± 0.12. A similar but more potent effect was observed for the BA-L fragment ($pEC_{50,diss}$ = 4.15 ± 0.25). These data suggest that the BA end of THRX-198321 binds to an allosteric site on M_3 receptors and that the linker plays a role in the interaction at that site.

The effects of THRX-198321 and THRX-198321 fragments on [^{3}H]NMS dissociation rates were also investigated at M_2 mAChR. In the absence of test compound, the M_2 [^{3}H]NMS dissociation $t_{1/2}$ was 3.4 ± 0.3 min and the apparent rate constant of dissociation k_{off} was 0.21 ± 0.02 min^{-1}. Similar to observations at the M_3 mAChR, THRX-198321, BA, and BA-L reduced dissociation rates of [^{3}H]NMS at M_2 mAChR; and $pEC_{50,diss}$ values were measured to be 6.73 ± 0.10, 2.77 ± 0.08, and 5.06 ± 0.03, respectively. Retardation of [^{3}H]NMS dissociation by THRX-198321 was inhibited by high concentrations of obidoxime (≥100 μM), a competitive inhibitor of allosteric modulator activities at M_2 mAChR (Ellis and Seidenberg, 1992; Tränkle and Mohr, 1997; Steinfeld et al., 2007). Concentration-effect curves for THRX-198321 were right-shifted in a parallel fashion with increasing concentrations of obidoxime (Fig. 5). A pA_2 value of 4.04 ± 0.73 was calculated for obidoxime, which is comparable with the value measured when tested with W84 in similar studies (Ellis and Seidenberg, 1992; Tränkle and Mohr, 1997; Steinfeld et al., 2007). The data fit best to the Lew and Angus model that describes a linear Schild plot with a slope factor less than 1 (slope = 0.73 ± 0.07). These data suggest that THRX-198321 binds to an allosteric site that overlaps with the common allosteric binding site defined by typical allosteric modulators such as gallamine and W84, that there is a degree of negative cooperativity between obidoxime and THRX-198321 or that data may be a composite of both activities. In other words, the orthosteric moiety of THRX-198321 may negatively modulate obidoxime binding at the allosteric site, yet the allosteric moiety occupies the "gallamine" allosteric site competitively.

The effects of THRX-198321 or MA on [^{3}H]DHA dissociation rates at β_2AR were also investigated. In studies using intact HEK-293 cells expressing β_2AR, high concentrations (≥100 μM) of THRX-198321 or MA were required to slow the dissociation of [^{3}H]DHA from the control rate ($t_{1/2}$ = 32 ± 9 min, k_{off} = 0.022 ± 0.007 min^{-1}). These data were generated using an EDTA buffer to inhibit cell aggregation. At the highest tested THRX-198321 concentration (1 mM), the k_{obs} was reduced to 0.0078 ± 0.0016 min^{-1}. The intrinsic solubility of THRX-198321 in this buffer system prevented testing at higher concentrations. The $pEC_{50,diss}$ values for THRX-198321 and MA were 3.82 ± 0.25 and 3.60 ± 0.27, respectively. The shape of the concentration response curves fit to a 4-parameter model in which the curve bottoms did not reach full inhibition of [^{3}H]DHA rate retardation (maximum inhibition ≈ 70%). These data are consistent with allosteric ligands interactions that are analogous to a partial agonist. A more modest effect was observed in similar studies using 1% BSA buffer to inhibit cell aggregation, where the [^{3}H]DHA dissociation rate measured in the presence of 1 mM THRX-198321 was slowed by approximately 2.5-fold relative to the control rate. THRX-198321 and the fragment MA slowed the rate of [^{3}H]DHA dissociation in a concentration-dependent manner. These data are consistent with the idea that the

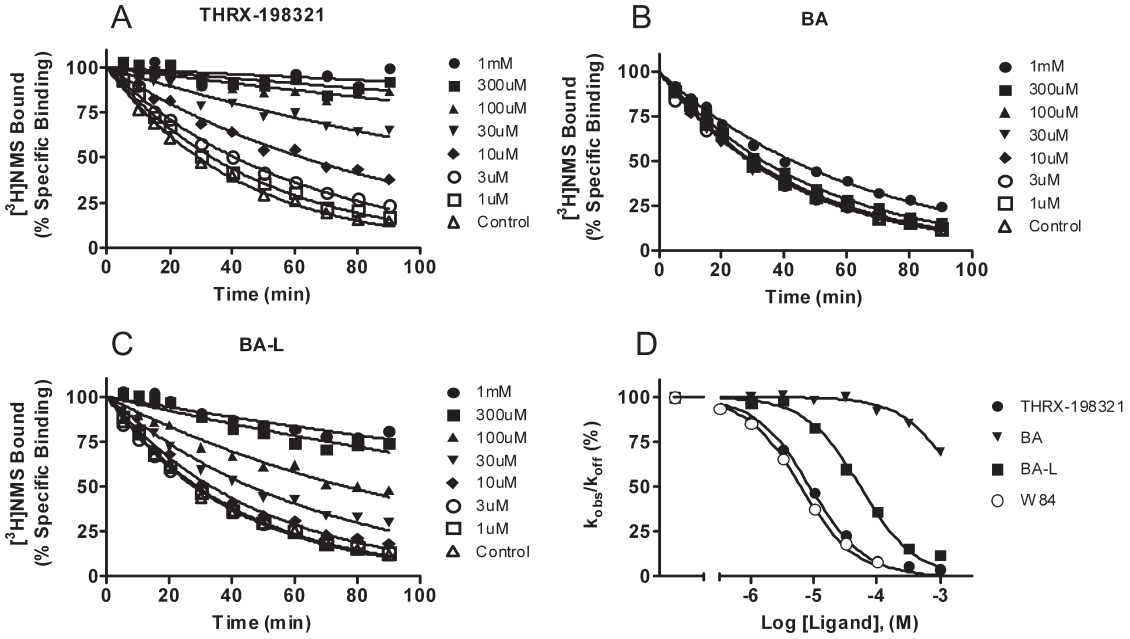

Fig. 4. Concentration-dependent effects of allosteric ligands on observed dissociation rates of [^{3}H]NMS from M_3 receptors. Dissociation of [^{3}H]NMS from human M_3 mAChR expressed in CHO-K1 cell membranes in the absence (△) or presence of 1 mM (●), 300 μM (■), 100 μM (▲), 30 μM (▼), 10 μM (◆), 3 μM (□), or 1 μM (□) THRX-198321 (A), BA (B), or BA-L (C). Curves represent the best fit of a monoexponential decay model. Data are representative of four separate experiments. D, concentration-effect curves were plotted from dissociation rate retardation studies for THRX-198321 (●), BA (▼), BA-L (■), and W84 (□). The observed dissociation rates (k_{obs}) were normalized to the percentage of the control dissociation rate (k_{off}) measured in the absence of test ligand and then fit to a four-parameter logistic equation.

MABA ligand can form a ternary complex with the radioligand and β_2AR before [^{3}H]DHA dissociation, supporting the claim that these ligands bind to an allosteric modulator site on β_2AR and that the allosteric site is extracellular (Fig. 6). In contrast, 1 mM BA had no effect on [^{3}H]DHA dissociation rates. Collectively, these data suggest the end of THRX-198321 that binds the β_2AR allosteric site is the moiety represented by MA. That the $pEC_{50,diss}$ values for THRX-198321 and MA are not significantly different suggests that MA is a pure allosteric ligand and that the linker and β_2AR orthosteric moieties play a negligible role in allosteric site binding.

MABA Binding Affinities and Quantification of Multivalent Effect Measured by Radioligand Inhibition Binding. In inhibition radioligand binding studies using CHO-K1 cell membrane fractions expressing M_2 or M_3 mAChR, THRX-198321 completely inhibited the binding of 1 nM [^{3}H]NMS at high concentrations (≥30 nM). The shapes of the inhibition curves for each receptor were similar, with slope factors close to unity. For all compounds tested, competitive interactions were assumed and IC_{50} values were converted to $pK_{I,App}$ values according to Cheng-Prusoff (1973), as summarized in Table 3. THRX-198321 bound tightly to M_2 and M_3 mAChR, with a modest degree of selectivity (3-fold) for M_2 receptors over M_3 receptors (M_2 $pK_{I,App}$ = 10.57 ± 0.09; M_3 $pK_{I,App}$ = 10.07 ± 0.11; $p < 0.001$). In general, THRX-198321 binding affinities were similar across the five muscarinic receptors. [THRX-198321 binding affinities ($pK_{I,App}$) measured using CHO-K1 cell membranes expressing human recombinant M_1, M_4, or M_5 receptors were determined to be 9.65 ± 0.20, 9.83 ± 0.08, or 9.00 ± 0.07, respectively.] At β_2AR, THRX-198321 also exhibited high affinity (Table 3). In contrast to the selectivity profile observed at muscarinic receptors, THRX-198321 was selective for β_2AR over β_1AR. [THRX-198321 binding affinity ($pK_{I,App}$) measured using HEK-293 cell membranes expressing human recombinant β_1-adrenoceptors was determined to be 7.12 ± 0.10].

To explore the multivalent properties of THRX-198321, the various truncated analogs were tested alone and in combination in the M_2 and M_3 mAChR and the β_2AR radioligand binding assays. MA exhibited higher affinity for M_2 and M_3 mAChR than β_2AR (M_2 $pK_{I,App}$ = 7.33 ± 0.20; M_3 $pK_{I,App}$ = 7.51 ± 0.12; β_2AR $pK_{I,App}$ = 4.94 ± 0.11), whereas BA demonstrated higher affinity for β_2AR than M_2 and M_3 mAChR (M_2 $pK_{I,App}$ = 5.07 ± 0.07; M_3 $pK_{I,App}$ = 4.50 ± 0.09; β_2AR $pK_{I,App}$ = 8.08 ± 0.08). For the linker-conjugated fragments MA-L and BA-L, $pK_{I,App}$ values were indistinguishable or similar to $pK_{I,App}$ values for the unconjugated fragments, except that for MA and MA-L at M_2, a difference in apparent affinity of approximately 10-fold was observed.

When the corresponding linker conjugated and unconjugated fragments (i.e., MA + BA-L or BA + MA-L) were coincubated, inhibition binding curve shapes did not deviate from one-site logistic models. Therefore, data were again analyzed assuming competitive inhibition of [^{3}H]NMS. The apparent affinity measurement for any pair of fragments did not differ significantly from the $pK_{I,App}$ value measured for the higher affinity frag-

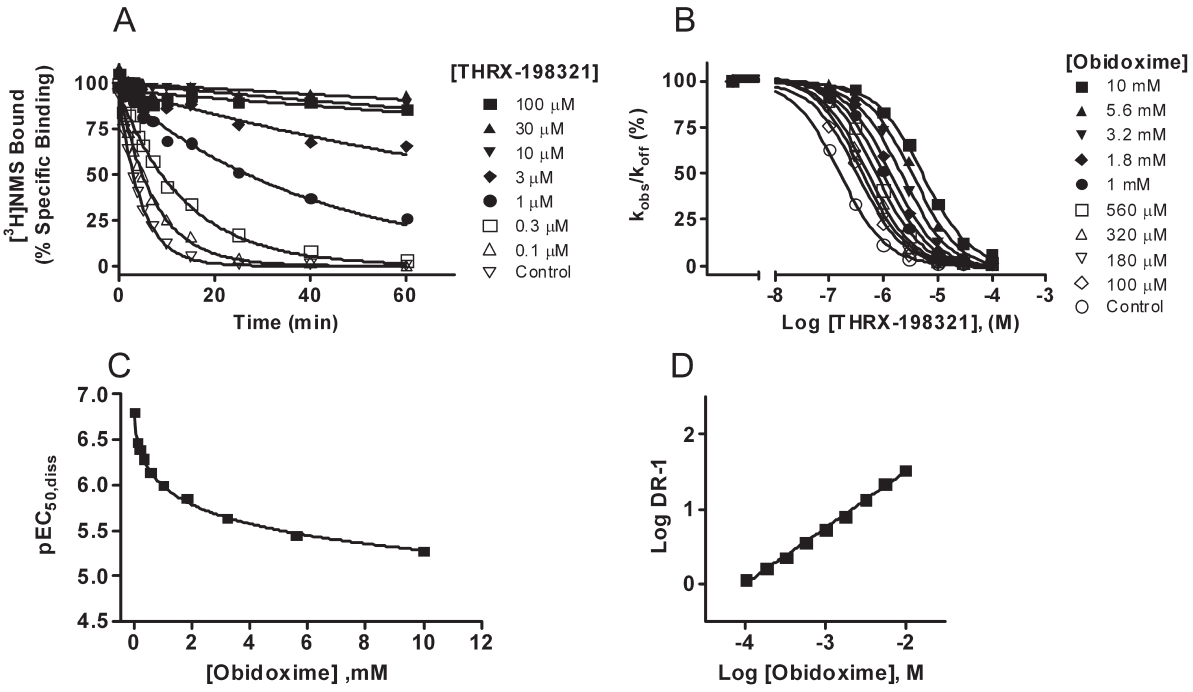

Fig. 5. Effects of obidoxime on THRX-198321 allosteric modulator activities at M_2 receptors. A, the dissociation rates of [^{3}H]NMS from human M_2 receptors expressed in CHO-K1 cell membranes was measured in the absence (◇) or presence of 100 (●), 30 (■), 10 (▲), 3 (▼), 1 (♦), 0.3 (□), or 0.1 μM (□) THRX-198321. Curves represent the best fit to a monoexponential decay model. Data, representative of four separate experiments, were normalized to the percentage of specific binding. B, observed dissociation rates (k_{obs}) were normalized to the percentage of the control dissociation rate (k_{off}) measured in the absence of obidoxime and plotted against the log concentration of THRX-198321. Concentration-effect curves measuring the THRX-198321 allosteric activity of [^{3}H]NMS dissociation rate retardation at human M_2 receptors were rightward shifted in the presence of 10 mM (●), 5.6 mM (■), 3.2 mM (▲), 1.8 mM (▼), 1 mM (♦), 560 μM (□), 320 μM (□), 180 μM (△), and 100 μM (▽) obidoxime, relative to concentration-effect curves measured in the absence of obidoxime (◇). Analyses of obidoxime-induced shifts in concentration-effect curves for THRX-198321 were performed using nonlinear regression (Lew and Angus, 1995) (C), and plotted against log concentration of obidoxime as a Schild regression (D) for visualization. Dose ratios were calculated by dividing the $EC_{50,diss}$ determined in the presence of obidoxime by the $EC_{50,diss}$ determined in the absence of obidoxime.

ment when assayed alone (Table 3). These data provide evidence for the multivalent mechanism of binding for THRX-198321, demonstrating that these pharmacophores must be linked to achieve subnanomolar activities.

To further explore the binding interaction of the carbamic acid moiety at the putative secondary site on β_2AR, a urea analog of THRX-198321 was synthesized and tested in the radioligand binding assays. The change of an oxygen in the carbamate moiety of THRX-198321 to a nitrogen in the urea analog (Fig. 7) resulted in apparent binding affinities that were 21-, 39-, and 62-fold weaker than THRX-198321 at M_2, M_3, and β_2, respectively (Table 4).

Analogs of THRX-198321 with varying linker lengths (C7–C12; Fig. 7) were synthesized and tested in the radioligand binding assays to explore the distances between orthosteric and allosteric sites located on β_2AR and mAChR, respectively. It is noteworthy that the C9 polymethylene linker in THRX-198321 was the optimal linker length for mAChRs and β_2AR (Fig. 8). For each linker analog, the rank order of affinities was M_2 mAChR > M_3 mAChR > β_2AR. The rank order of affinities at M_2 and M_3 mAChR was THRX-198321 > C10 > C8 > C11 > C7 > C12, whereas the rank order of affinities at β_2AR was THRX-198321 > C7 = C8 = C10 > C11 > C12 (Table 4).

Ligand binding free energies were calculated from apparent inhibition binding constants using the equation, ΔG =

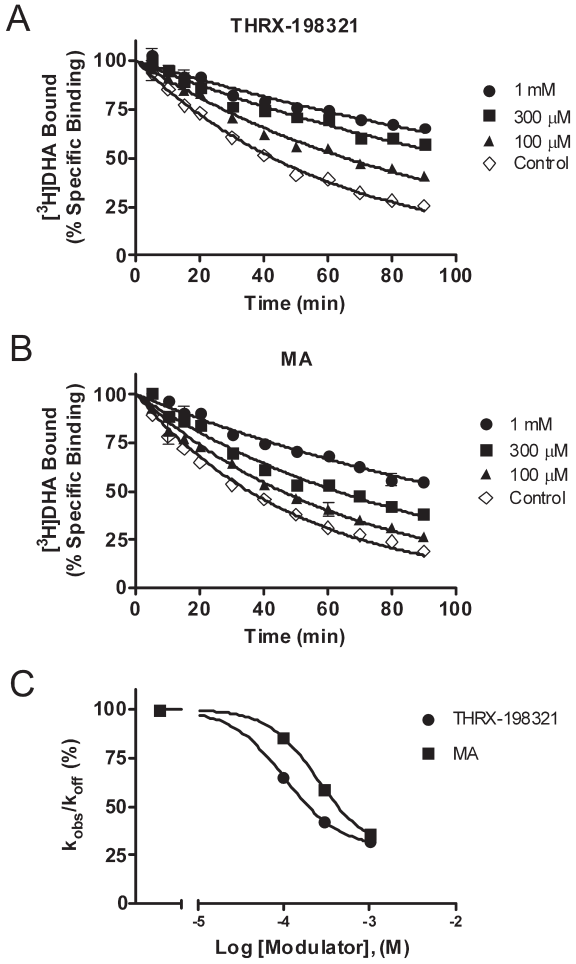

Fig. 6. Concentration-dependent effects of allosteric ligands on observed dissociation rates of [^{3}H]DHA from β_2AR expressed in intact HEK-293 cells. Dissociation of [^{3}H]DHA from β_2AR in the absence (◇) or presence of 1 mM (●), 300 μM (■), or 100 μM (▲) THRX-198321 (A) or MA (B). Curves represent the best fit of a monoexponential decay model. Data are representative of three separate experiments. Before analysis, data were normalized to the percentage of specific binding. Concentration-effect curves were plotted from dissociation rate retardation studies for THRX-198321 (●) or MA (▲), C, the observed dissociation rates (k_{obs}) were normalized to the percentage of the control dissociation rate (k_{off}) measured in the absence of test ligand and were fit to a four-parameter logistic equation.

TABLE 3

Apparent inhibition binding constants ($pK_{I,App}$) for THRX-198321 and THRX-198321 fragments at M_2 and M_3 mAChR and β_2AR

Apparent inhibition binding constants for THRX-198321 or THRX-198321 fragments alone or in combination at CHO-K1 cell membranes expressing M_2 mAChR, CHO-K1 cell membranes expressing M_3 mAChR, and HEK-293 cell membranes expressing β_2AR were determined using conventional [^{3}H]NMS or [^{3}H]DHA inhibition radioligand binding assays. Competitive binding interactions between test ligand and radioligand were assumed, thus IC_{50} values were converted to $pK_{I,App}$ values according to Cheng-Prusoff. Mean values ± S.D. are derived from four separate experiments performed in duplicate.

	$pK_{I,App}$		
	M_2	M_3	β_2AR
THRX-198321	10.57 ± 0.09	10.07 ± 0.11	9.54 ± 0.15
MA	7.33 ± 0.20	7.51 ± 0.12	4.94 ± 0.11
MA-L	8.20 ± 0.25	7.94 ± 0.21	4.54 ± 0.22
BA	5.07 ± 0.07	4.50 ± 0.09	8.08 ± 0.08
BA-L	4.87 ± 0.07	4.69 ± 0.06	8.21 ± 0.03
MA + BA-L	7.17 ± 0.05[a]	7.47 ± 0.12[a]	8.21 ± 0.07[b]
MA-L + BA	8.45 ± 0.10[c]	7.92 ± 0.28[c]	7.97 ± 0.05[d]
MA + BA	7.28 ± 0.04[a]	7.44 ± 0.13[a]	8.01 ± 0.04[b]

[a] Value for coincubated fragments was not significantly different from value for MA when tested alone ($P < 0.05$).
[b] Value for coincubated fragments was not significantly different from value for BA-L when tested alone ($P < 0.05$).
[c] Value for coincubated fragments was not significantly different from value for MA-L when tested alone ($P < 0.05$).
[d] Value for coincubated fragments was not significantly different from value for MA when tested alone ($P < 0.05$).

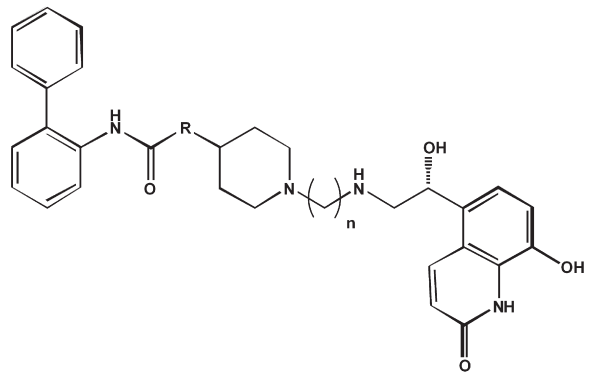

THRX-198321 Analog	R	n
C7	O	7
C8	O	8
C10	O	10
C11	O	11
C12	O	12
Urea	NH	9

Fig. 7. THRX-198321 analogs used to systematically evaluate the impact of linker length and carbamate replacement on binding affinities.

$-R \cdot T \ln(K_{I,App})$,where R is the gas constant (1.98×10^{-3} kcal $\cdot$ mol$^{-1} \cdot$ K^{-1}) and T is temperature (310 K). For THRX-198321, free energy values were calculated to be 14.9, 14.2, and 13.5 kcal/mol for M_2, M_3 mAChR, and β_2AR, respectively. These values are summarized in Table 5. Sums of individual values for fragment pairs are also reported for comparison. For the pair of THRX-198321 fragments lacking the linker extension (MA and BA), the sums of free energies were calculated to be 17.5, 17.0, and 18.4 kcal/mol for M_2, M_3 mAChR, and β_2AR, respectively. The binding energy for the urea analog of THRX-198321 was 11.0 kcal/mol, a decrease in binding energy of 2.5 kcal/mol relative that for THRX-198321 at β_2AR.

TABLE 4

Apparent inhibition binding constants ($pK_{I,App}$) for THRX-198321 analogs at M_2 and M_3 mAChR and β_2AR

Apparent inhibition binding constants for THRX-198321 analogs measured at CHO-K1 cell membranes expressing M_2 mAChR, CHO-K1 cell membranes expressing M_3 mAChR, and HEK-293 cell membranes expressing β_2AR were determined using conventional [^{3}H]NMS or [^{3}H]DHA inhibition radioligand binding assays. The linker length refers to the number of methylene units separating the MA and BA moieties. Mean values ± S.D. are derived from four separate experiments.

	$pK_{I,App}$		
	M_2	M_3	β_2
C7 linker	9.54 ± 0.11	9.13 ± 0.03	8.93 ± 0.07
C8 linker	9.89 ± 0.09	9.49 ± 0.03	8.92 ± 0.23
THRX-198321	10.57 ± 0.09	10.07 ± 0.11	9.54 ± 0.15
C10 linker	9.98 ± 0.12	9.60 ± 0.08	8.87 ± 0.24
C11 linker	9.77 ± 0.13	9.35 ± 0.19	8.56 ± 0.30
C12 linker	9.50 ± 0.12	8.90 ± 0.11	8.14 ± 0.04
Urea	9.24 ± 0.06	8.48 ± 0.06	7.75 ± 0.07

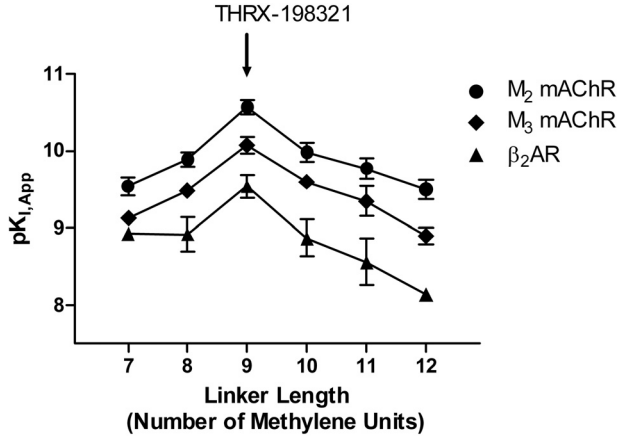

Fig. 8. Linker length dependence on apparent binding affinities at M_2 mAChR, M_3 mAChR. and β_2AR. Negative log values of apparent inhibition constants ($pK_{I,App}$) were measured at CHO-K1 cell membranes expressing M_2 mAChR, CHO-K1 cell membranes expressing M_3 mAChR, and HEK-293 cell membranes expressing β_2AR and plotted against the number of methylene units contained in the linker moiety for THRX-198321 and THRX-198321 linker analogs. Connecting lines were drawn for M_2 mAChR (■), M_3 mAChR (▲), and β_2AR (●) to better visualize the trends.

TABLE 5

Calculated binding free energy values for THRX-198321 and THRX-198321 fragments at M_2 and M_3 mAChR and β_2AR

Binding free energy values were calculated from $K_{I,App}$ values using the formula $\Delta G = -R \cdot T \ln(K_{I,App})$. $K_{I,App}$ values measured at CHO-K1 cell membranes expressing M_2 mAChR, CHO-K1 cell membranes expressing M_3 mAChR, and HEK-293 cell membranes expressing β_2AR were determined using typical [^{3}H]NMS or [^{3}H]DHA inhibition radioligand binding assays (see Table 3).

	M_2	M_3	β_2AR
		kcal/mol	
THRX-198321	14.9	14.2	13.5
MA	10.4	10.6	7.0
MA-L	11.6	11.2	6.4
BA	7.2	6.4	11.4
BA-L	6.9	6.6	11.6
Urea analog	13.1	12.0	11.0

Discussion

In the present study, we have described the pharmacological profile of a novel, potent dual pharmacology ligand, THRX-198321, discovered using a multivalent design strategy. THRX-198321 was chosen as a tool for the present study as a representative MABA exhibiting muscarinic receptor antagonist and beta adrenoceptor agonist properties. The pharmacological activities and binding modes of THRX-198321 were examined at M_2 mAChR, M_3 mAChR, and β_2AR, receptors, which are relevant to smooth muscle contraction and modulation of bronchodilation.

The design of multivalent ligands for GPCRs has been described previously (Disingrini et al., 2006; Steinfeld et al., 2007; Valant et al., 2008; Antony et al., 2009; Kebig et al., 2009); however, here concepts in multivalency were extended to introduce dual pharmacology, an atypical characteristic of multivalent ligands. The dual pharmacological activity of THRX-198321 is attributed to structural elements found within the ligand. The BA moiety contains a carbostyril core, a well characterized β_2AR agonist pharmacophore (Yoshizaki et al., 1976; Milecki et al., 1987). The biphenyl carbamic acid moiety, represented by MA, is of a class of compounds that has been reported as mAChR antagonists (Naito et al., 1998a,b). Truncated THRX-198321 fragments retained their respective pharmacological activities as confirmed using assays designed to measure functional agonism or antagonism. Covalent linkage of these fragments by a C9 polymethylene chain resulted in a single molecule exhibiting potent mAChR antagonist and β_2AR agonist activities.

THRX-198321 exhibits three characteristics of binding interactions that are consistent with multivalent interactions: 1) multiple binding interactions at a given receptor, 2) enhanced binding affinity for the multivalent ligand relative to monovalent fragments, and 3) a quantifiable multivalent effect. These are discussed in further detail in the sections that follow.

THRX-198321 and the MA moiety were competitive with the mAChR agonist oxotremorine, providing evidence that the MA moiety of THRX-198321 binds to the mAChR orthosteric site. Kinetic data (retardation of [^{3}H]NMS dissociation rates) provide evidence that THRX-198321 can cobind to the mAChR when occupied by the orthosteric radioligand, suggesting that THRX-198321 binds to a mAChR allosteric site. The specificity of this allosteric interaction at M_2 was confirmed using the allosteric modulator inhibitor obidoxime, which also provided evidence that THRX-198321 binds to a region on M_2 receptors coincident with other typical allosteric modulators, such as gallamine and W84 (Ellis and Seidenberg, 1992; Tränkle and Mohr, 1997; Steinfeld et al., 2007). A similar study showing the interaction between obidoxime and the mAChR allosteric moiety of THRX-198321, BA, could not be performed because the potency of BA in this assay was too weak. Formation of a ternary complex of [^{3}H]NMS, THRX-198321 (or BA), and M_3 mAChR also was observed;

however, the low potency of obidoxime at this receptor prevented identification of the specific allosteric site. Therefore, it can only be assumed that the allosteric binding pocket on M_3 receptors that binds THRX-198321 is homologous to the obidoxime allosteric site on M_2 receptors. It is of particular interest to note that a prototypical β_2AR agonist pharmacophore, such as the carbostyril-containing BA fragment, functions as an allosteric modulator of mAChR and serves as a secondary binding anchor for THRX-198321.

Before this report, the only known allosteric modulator for the β_2AR was Zn^{2+}, the binding site for which seems to be located on the third cytoplasmic loop of the receptor (Swaminath et al., 2003). Here we report the first evidence for an allosteric interaction at β_2AR using a small synthetic ligand, the binding site for which seems to be extracellular. THRX-198321 and MA slowed the dissociation rate of [^{3}H]DHA from β_2AR in a manner consistent with an allosteric interaction. That these studies were performed using intact cells suggests that the allosteric site that binds THRX-198321 and MA is extracellular and thus distinct from the Zn^{2+} allosteric binding site previously reported. The potency of MA is consistent with binding energies sufficient to increase binding affinity of BA in a multivalent capacity. These data are consistent with the hypothesis that the MA moiety of THRX-198321 binds to a novel allosteric site on β_2AR, the location of which remains to be identified.

The β_2AR agonist activities of THRX-198321 and, more specifically, BA, are competitively inhibited by propranolol, supporting our hypothesis that the carbostyril moiety of THRX-198321 binds to the β_2AR orthosteric site. These data, taken together with the kinetic data, support the hypothesis that THRX-198321 binds to distinct orthosteric and allosteric sites on β_2AR in a multivalent manner.

We demonstrated enhanced binding affinity for the multivalent ligand, THRX-198321, relative to monovalent fragments at mAChR. That mAChR binding affinities are increased approximately 2 orders of magnitude when MA is covalently linked to BA, to form THRX-198321, supports the hypothesis that THRX-198321 is a multivalent ligand. This conclusion is corroborated by observed increases in functional antagonist potencies for THRX-198321 relative to THRX-198321 fragments. Radioligand binding data for the linker-conjugated fragments suggest that the linker may play a significant role in receptor binding. However, as discussed previously (Steinfeld et al., 2007), the gains in mAChR binding affinity for the linker conjugated fragments (e.g., MA-L relative to MA) are believed to represent overestimates of the linker contribution to enhancement of the receptor binding affinity.

Increases in binding affinity for the multivalent ligand relative to the monovalent fragments were also observed at β_2AR; however, these were more modest than observed at mAChRs. These data suggest that although there is positive cooperativity between MA and BA fragments at both mAChR and β_2AR, the cooperativity is greater in magnitude at M_2 and M_3 mAChR than at β_2AR.

To quantify the multivalent effect for THRX-198321, binding free energies were calculated from apparent binding affinities. The sum of free energies for THRX-198321 fragments represents the upper bound of the free energy of binding of THRX-198321, assuming the maximum possible multivalent effect. However, several important factors prohibit a quantitative assessment here. First, because the mode of binding for the linker-conjugated fragments may not exactly mimic the mode of binding for the MABA, the reported binding data may overestimate the contribution of the linker-conjugated fragment. Conversely, the linker may contribute to the binding energy through direct contact with the receptor. Second, the sum of the free energies of the fragments measured independently does not account for interaction terms (cooperativity, either positive or negative). Furthermore, cooperativities between allosteric fragments and orthosteric radioligands may not accurately represent cooperativities between allosteric and orthosteric fragments of THRX-198321.

In addition to providing information regarding the multivalent nature of THRX-198321, binding free-energy data may also quantify the importance of binding to a given binding pocket. At β_2AR, the apparent binding affinities for BA and the urea analog of THRX-198321 were similar, suggesting that the binding energy for the urea analog at β_2AR is derived largely, if not entirely, from the BA moiety. The 2.5 kcal/mol gain in binding energy for THRX-198321 relative to the urea analog at β_2AR represents a significant gain in binding energy that is consistent with the idea that the carbamic acid moiety of THRX-198321 occupies a secondary site on β_2AR. It is noteworthy that structural differences between the carbamic acid and urea are minor, suggesting that binding at the β_2AR allosteric site is highly sensitive to small structural changes.

The data presented here are consistent with the notion that THRX-198321 binds in a multivalent manner at both mAChR and β_2AR and that the orientation of THRX-198321 relative to orthosteric and allosteric sites is bimodal (Fig. 9). By extension, it should be possible to define distinct structure-activity relationships at both the orthosteric and allosteric binding pockets on mAChR and β_2AR that bind THRX-198321. To the best of our knowledge, the phenomenon of bimodal binding at GPCRs is unprecedented.

It is interesting to speculate as to why it might be possible for a MABA to bind in the modes described. A more specific inquiry might be made to understand why a β_2AR agonist serves as a binding anchor at an allosteric site on mAChRs for THRX-198321. Receptor "specific" ligands can be integrated into a multivalent ligand almost interchangeably, which suggests that there are similarities to be considered, at least within these specific binding regions. Moreover, the spatial relationship between the orthosteric and allosteric

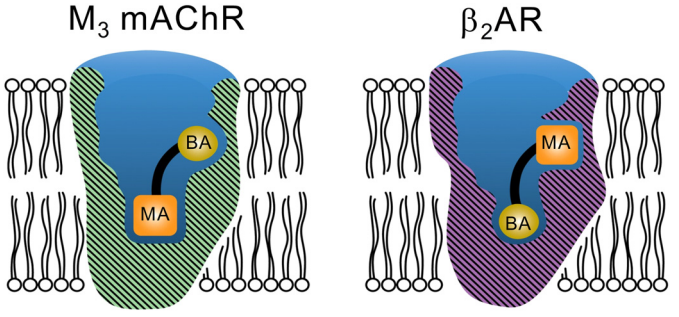

Fig. 9. Cartoon depicting the multivalent modes of binding for THRX-198321 at mAChR (M) and β_2AR. Our data suggest that THRX-198321 exhibits bimodal binding at these receptors, where the mAChR orthosteric moiety MA binds to a novel allosteric site on β_2AR. Likewise, the β_2AR orthosteric moiety BA binds to the mAChR allosteric site coincident with other typical mAChR allosteric modulators, such as W84.

sites on these receptors seems to be similar. It is possible that mAChR and β_2AR are more similar than previously thought. This is little more than speculation in the absence of mutagenesis data showing the location of the β_2AR allosteric site and comparisons with sites identified on mAChR. However, our data may begin to shed light on what may be evolutionary relationships between these receptors. Many questions remain unanswered, but it is hoped that this work will stimulate further studies and debate.

From a therapeutic perspective, our discovery of MABA ligands was the combined result of successes in multivalent drug design and respiratory disease research that represents a potential major breakthrough in novel therapies for COPD. A single molecule exhibiting dual pharmacological activities represents a novel approach toward the discovery of bronchodilators. Several MABAs are currently being clinically evaluated, the most advanced being GSK961081 (TD-5959). The combined activities of a MABA may result in synergistic increases in bronchodilation and therefore offer the potential for superior efficacy relative to therapies with a single activity and may make triple therapy with a corticosteroid, for example, more feasible.

Acknowledgments

We thank Jill Steinfeld for preparing the illustration of the interactions between receptors and the multivalent MABA ligand.

Authorship Contributions

Participated in research design: Steinfeld, Klein, Smith, and Mammen.

Conducted experiments: Steinfeld.

Contributed new reagents or analytic tools: Hughes.

Performed data analysis: Steinfeld.

Wrote or contributed to the writing of the manuscript: Steinfeld, Hughes, Klein, Smith, and Mammen.

References

Aaron SD, Vandemheen KL, Fergusson D, Maltais F, Bourbeau J, Goldstein R, Balter M, O'Donnell D, McIvor A, Sharma S, et al. (2007) Tiotropium in combination with placebo, salmeterol, or fluticasone-salmeterol for treatment of chronic obstructive pulmonary disease: a randomized trial. *Ann Intern Med* **146:**545–555.

Antony J, Kellershohn K, Mohr-Andrä M, Kebig A, Prilla S, Muth M, Heller E, Disingrini T, Dallanoce C, Bertoni S, et al. (2009) Dualsteric GPCR targeting: a novel route to binding and signaling pathway selectivity. *FASEB J* **23:**442–450.

Arch JR, Ainsworth AT, Cawthorne MA, Piercy V, Sennitt MV, Thody VE, Wilson C, and Wilson S (1984) Atypical beta-adrenoceptor on brown adipocytes as target for anti-obesity drugs. *Nature* **309:**163–165.

Arunlakshana O and Schild HO (1959) Some quantitative uses of drug antagonists. *Br J Pharmacol Chemother* **14:**48–58.

Baker WL, Baker EL, and Coleman CI (2009) Pharmacologic treatments for chronic obstructive pulmonary disease: a mixed-treatment comparison meta-analysis. *Pharmacotherapy* **29:**891–905.

Baloira Villar A and Vilariño Pombo C (2005) [Bronchodilator efficacy of combined salmeterol and tiotropium in patients with chronic obstructive pulmonary disease]. *Arch Bronconeumol* **41:**130–134.

Calverley PM (2004) Reducing the frequency and severity of exacerbations of chronic obstructive pulmonary disease. *Proc Am Thorac Soc* **1:**121–124.

Cazzola M, Centanni S, Santus P, Verga M, Mondoni M, di Marco F, and Matera MG (2004) The functional impact of adding salmeterol and tiotropium in patients with stable COPD. *Respir Med* **98:**1214–1221.

Cheng Y and Prusoff WH (1973) relationship between the inhibition constant (K1) and the concentration of inhibitor which causes 50 per cent inhibition (I50) of an enzymatic reaction. *Biochem Pharmacol* **22:**3099–3108.

Disingrini T, Muth M, Dallanoce C, Barocelli E, Bertoni S, Kellershohn K, Mohr K, De Amici M, and Holzgrabe U (2006) Design, synthesis, and action of oxotremorine-related hybrid-type allosteric modulators of muscarinic acetylcholine receptors. *J Med Chem* **49:**366–372.

Ellis J and Seidenberg M (1992) Two allosteric modulators interact at a common site on cardiac muscarinic receptors. *Mol Pharmacol* **42:**638–641.

Green SA, Spasoff AP, Coleman RA, Johnson M, and Liggett SB (1996) Sustained activation of a G protein-coupled receptor via "anchored" agonist binding. Molecular localization of the salmeterol exosite within the 2-adrenergic receptor. *J Biol Chem* **271:**24029–24035.

Griffin JH, Linsell MS, Nodwell MB, Chen Q, Pace JL, Quast KL, Krause KM, Farrington L, Wu TX, Higgins DL, et al. (2003) Multivalent drug design. Synthesis and in vitro analysis of an array of vancomycin dimers. *J Am Chem Soc* **125:**6517–6531.

Kebig A, Kostenis E, Mohr K, and Mohr-Andrä M (2009) An optical dynamic mass redistribution assay reveals biased signaling of dualsteric GPCR activators. *J Recept Signal Transduct Res* **29:**140–145.

Leff P and Dougall IG (1993) Further concerns over Cheng-Prusoff analysis. *Trends Pharmacol Sci* **14:**110–112.

Lew MJ and Angus JA (1995) Analysis of competitive agonist-antagonist interactions by nonlinear regression. *Trends Pharmacol Sci* **16:**328–337.

Long DD, Aggen JB, Christensen BG, Judice JK, Hegde SS, Kaniga K, Krause KM, Linsell MS, Moran EJ, and Pace JL (2008) A multivalent approach to drug discovery for novel antibiotics. *J Antibiot* (*Tokyo*) **61:**595–602.

Mammen M, Choi SK, and Whitesides GM (1998a) Polyvalent interactions in biological systems: implications for design and use of multivalent ligands and inhibitors. *Angew Chem Int Ed* **37:**2754–2794.

Mammen M, Shakhnovich EI, and Whitesides GM (1998b) Using a convenient, quantitative model for torsional entropy to establish qualitative trends for molecular processes that restrict conformational freedom. *J Org Chem* **63:**3168–3175.

Mathers CD and Loncar D (2006) Projections of global mortality and burden of disease from 2002 to 2030. *PLoS Med* **3:**e442.

May LT, Leach K, Sexton PM, and Christopoulos A (2007) Allosteric modulation of G protein-coupled receptors. *Annu Rev Pharmacol Toxicol* **47:**1–51.

McKinnell RM, Armstrong SR, Beattie DT, Choi SK, Fatheree PR, Gendron RA, Goldblum A, Humphrey PP, Long DD, Marquess DG, et al. (2009) A multivalent approach to the design and discovery of orally efficacious 5-HT4 receptor agonists. *J Med Chem* **52:**5330–5343.

Milecki J, Baker SP, Standifer KM, Ishizu T, Chida Y, Kusiak JW, and Pitha J (1987) Carbostyril derivatives having potent beta-adrenergic agonist properties. *J Med Chem* **30:**1563–1566.

Naito R, Takeuchi M, Morihira K, Hayakawa M, Ikeda K, Shibanuma T, and Isomura Y (1998a) Selective muscarinic antagonists. I. Synthesis and antimuscarinic properties of 4-piperidyl benzhydrylcarbamate derivatives. *Chem Pharm Bull* (*Tokyo*) **46:**1274–1285.

Naito R, Takeuchi M, Morihira K, Hayakawa M, Ikeda K, Shibanuma T, and Isomura Y (1998b) Selective muscarinic antagonists. II. Synthesis and antimuscarinic properties of biphenylylcarbamate derivatives. *Chem Pharm Bull* (*Tokyo*) **46:**1286–1294.

Smith C and Teitler M (1999) Beta-blocker selectivity at cloned human beta 1- and beta 2-adrenergic receptors. *Cardiovasc Drugs Ther* **13:**123–126.

Smith JA, Amagasu SM, Hembrador J, Axt S, Chang R, Church T, Gee C, Jacobsen JR, Jenkins T, Kaufman E, et al. (2006) Evidence for a multivalent interaction of symmetrical, N-linked, lidocaine dimers with voltage-gated Na^+ channels. *Mol Pharmacol* **69:**921–931.

Steinfeld T, Mammen M, Smith JA, Wilson RD, and Jasper JR (2007) A novel multivalent ligand that bridges the allosteric and orthosteric binding sites of the M2 muscarinic receptor. *Mol Pharmacol* **72:**291–302.

Swaminath G, Lee TW, and Kobilka B (2003) Identification of an allosteric binding site for Zn^{2+} on the beta2 adrenergic receptor. *J Biol Chem* **278:**352–356.

Swaminath G, Steenhuis J, Kobilka B, and Lee TW (2002) Allosteric modulation of beta2-adrenergic receptor by Zn^{2+}. *Mol Pharmacol* **61:**65–72.

Tashkin DP, Littner M, Andrews CP, Tomlinson L, Rinehart M, and Denis-Mize K (2008) Concomitant treatment with nebulized formoterol and tiotropium in subjects with COPD: a placebo-controlled trial. *Respir Med* **102:**479–487.

Tränkle C and Mohr K (1997) Divergent modes of action among cationic allosteric modulators of muscarinic M2 receptors. *Mol Pharmacol* **51:**674–682.

Valant C, Gregory KJ, Hall NE, Scammells PJ, Lew MJ, Sexton PM, and Christopoulos A (2008) A novel mechanism of G protein-coupled receptor functional selectivity. Muscarinic partial agonist McN-A-343 as a bitopic orthosteric/allosteric ligand. *J Biol Chem* **283:**29312–29321.

van Noord JA, Aumann JL, Janssens E, Smeets JJ, Verhaert J, Disse B, Mueller A, and Cornelissen PJ (2005) Comparison of tiotropium once daily, formoterol twice daily and both combined once daily in patients with COPD. *Eur Respir J* **26:**214–222.

van Noord JA, Aumann JL, Janssens E, Verhaert J, Smeets JJ, Mueller A, and Cornelissen PJ (2006) Effects of tiotropium with and without formoterol on airflow obstruction and resting hyperinflation in patients with COPD. *Chest* **129:**509–517.

Yoshizaki S, Tanimura K, Tamada S, Yabuuchi Y, and Nakagawa K (1976) Sympathomimetic amines having a carbostyril nucleus. *J Med Chem* **19:**1138–1142.

Address correspondence to: Tod Steinfeld, Department of Molecular and Cellular Biology, Theravance, Inc., 901 Gateway Blvd., South San Francisco, CA 94080. E-mail: tsteinfeld@theravance.com